Multiple state transition path sampling

Rogal, J.; Bolhuis, P.G.

DOI
10.1063/1.3029696
Publication date
2008

Published in
Journal of Chemical Physics

Multiple state transition path sampling

Jutta Rogal[a] and Peter G. Bolhuis
Van't Hoff Institute for Molecular Sciences, University of Amsterdam, Nieuwe Achtergracht 166, 1018 WV Amsterdam, The Netherlands

(Received 31 July 2008; accepted 30 October 2008; published online 10 December 2008)

We developed a multiple state transition path sampling (TPS) approach in which it is possible to simultaneously sample pathways connecting a number of different stable states. Based on the original formulation of the TPS we have extended the path ensemble to include trajectories connecting not only two distinct stable states but any two states defined within a system. The multiple state TPS approach is useful in complex systems exhibiting a number of intermediate stable states that are interconnected in phase space. Combining this approach with transition interface sampling we can also directly obtain an expression for the rate constants of all possible transitions within the system. © *2008 American Institute of Physics*. [DOI: 10.1063/1.3029696]

I. INTRODUCTION

The dynamical properties of complex systems are often characterized by the existence of several stable or metastable states that are separated by large free energy barriers. Examples for such complex systems are omnipresent throughout nature varying from conformational changes in biological relevant molecules to phase transitions as well as many chemical reactions. The long time behavior of such systems is usually determined by transitions between stable states, e.g., conformational or structural changes. Due to large free energy barriers between stable states these transitions are very rare compared to the short time dynamics (e.g., vibrations) within each of the stable states resulting in a separation of time scales. This so-called time scale problem makes it unfeasible to study such a system over an extended time scale with regular molecular dynamics (MD) simulations.

One possibility to address this problem is the use of a biasing potential along a set of order parameters. Several computational techniques have been developed in this area, e.g., umbrella sampling,[1] blue moon sampling,[2] hyperdynamics,[3] and metadynamics.[4] The main drawback of these techniques is the choice of order parameters. If the order parameters do not provide a good approximation to the true reaction coordinate these methods fail.

A different possibility to examine the dynamical behavior on an extended time scale is to coarse grain the system. This approach concentrates on the rare events only, i.e., the transitions between stable states, and describes the time evolution within a Markovian state model (MSM).[5–7] The short time dynamics within each stable state are appropriately averaged and accounted for in the corresponding transition probabilities.

After a proper identification of the different stable states the essential ingredients of a MSM are the rate constants, respectively, transition probabilities that characterize the transition between the stable states. These rate constants are not trivial to obtain since again straightforward MD simulations are usually impracticable. One approach is to use transition path sampling[8] (TPS) or the more efficient transition interface sampling[9] (TIS) for the computation of the rate constants. TPS has successfully been applied to study a variety of different systems ranging from crystal nucleation[10] to the folding of small proteins[11] (for an overview of applications in biological systems, cf. Ref. 12) and transformation of nanoparticles under pressure.[13] However, in these path sampling methods the sampling is restricted to pathways connecting only two distinct stable states. In complex systems with several intermediate stable states the sampling of the path space can become very inefficient since trajectories might get stuck in intermediate states, i.e., the escape from the intermediate state is a rare event in itself. The sampling of such long trajectories crossing intermediate states can be enhanced by the precision shooting algorithm recently introduced by Grünwald *et al.*[14] While this algorithm can produce slightly modified pathways that remain reactive it is not expected to provide reactive trajectories that substantially differ within the intermediate state as required for a proper sampling of path space. A simple alternative is to perform a separate TPS simulation for each subreaction.[15] However, for N stable states this requires $N(N-1)$ simulations and can still be very inefficient due to rejection of pathways that do not start and end in the selected states.

To address this problem we have extended the TPS method to multiple stable states instead of including only two distinct stable states in the path ensemble. Applying such a multiple state TPS approach we can now sample pathways that connect any two stable or intermediate states in our system within one single simulation. Based on the rate constant formulation in TIS we obtain an expression for the rate constants of all possible transitions between all of the stable or metastable states in the system.

In this paper we introduce the formalism of multiple state TPS and test this method on two simple characteristic model systems using both stochastic and deterministic dynamics. This paper is organized as follows. In Sec. II a formal derivation of the multiple state TPS is given. In Sec. III the application of the method to the two model systems is

[a]Electronic mail: j.g.rogal@uva.nl.

discussed. The first model system represents a diffusive system with several stable states explored using Langevin dynamics (LD). In the second model system deterministic dynamics are used. At the end of Sec. III we discuss some further developments to improve the current method. A summary is given in Sec. IV.

II. THEORETICAL BACKGROUND

We first review very briefly the basic ideas of TPS and TIS that we then extend from two-state systems to multiple states. An extensive discussion of the two methods can be found in Refs. 8 and 9.

A. Transition path sampling

In TPS (Ref. 8) a properly weighted set of reactive trajectories is explored by performing a random walk in trajectory space. The pathways are reactive in a sense that they connect two distinct states in a given system which are usually referred to as the initial and final states although, in principle, the pathways are always entirely reversible. The path ensemble of trajectories starting in a defined region A and ending in region B is given by

$$\mathcal{P}_{AB}[\mathbf{x}(L)] \equiv Z_{AB}^{-1} h_A(x_0) \mathcal{P}[\mathbf{x}(L)] h_B(x_L), \tag{1}$$

where Z_{AB} is a normalization factor and $h_A(x)$ and $h_B(x)$ are characteristic functions defining states A and B, i.e., they are equal to one if the configuration x is within the state and zero if it is outside. $\mathcal{P}[\mathbf{x}(L)]$ is the dynamical path probability for a discretized path $\mathbf{x}(L)=\{x_0, x_{\Delta t}, \ldots, x_{L\Delta t}\}$ of fixed length $L\Delta t$,

$$\mathcal{P}[\mathbf{x}(L)] = \rho(x_0) \prod_{\tau=0}^{L-1} p(x_\tau \to x_{(\tau+1)}) \tag{2}$$

given by the distribution of initial conditions $\rho(x_0)$ and the product over the Markovian short time transition probabilities[16] to evolve a time slice x_τ for a certain time Δt into the next slice $x_{\tau+1}$ with τ being the discrete time index $\tau=t/\Delta t$. Each time slice x_τ contains all positions and momenta of all particles in the system at time $t=\tau\Delta t$, i.e., $x_\tau=\{\mathbf{r}_\tau, \mathbf{p}_\tau\}$. To sample the path space the shooting algorithm is used. In this algorithm a time slice is chosen from the trajectory which is then changed, e.g., by perturbing the current momenta and/or positions, and a new pathway is created by generating new forward and backward segments from this modified time slice. Since the path ensemble consists of true dynamical trajectories it is in principle possible to extract dynamical properties of the system such as rate constants though in practice this can become rather time consuming.

B. Transition interface sampling

TIS (Ref. 9) is an efficient TPS based algorithm for the calculation of rate constants. In addition to defining the initial and final state regions an order parameter λ is needed. This order parameter does not have to reflect the true reaction coordinate of the system, but it has to clearly distinguish between the two states, either monotonically increasing or decreasing. Using the order parameter λ interfaces are defined as hypersurfaces $\{x:\lambda(x)=\lambda_s\}$ with $\lambda_s \in \mathbb{R}$. Within the TIS method the rate constant for the transition from a state A to a state B can be expressed as the flux $\langle \phi_0 \rangle$ through the first interface $\lambda_0=\lambda_A$ that also defines the stable state region A, multiplied with the crossing probability $P_A(\lambda_B|\lambda_0)$,

$$k_{AB} = \langle \phi_0 \rangle P_A(\lambda_B|\lambda_0) = \langle \phi_0 \rangle \prod_{s=0}^{n-1} P_A(\lambda_{s+1}|\lambda_s). \tag{3}$$

The crossing probability is the probability that whenever λ_0 is crossed λ_B will be crossed before returning to A, i.e., before crossing λ_0 again. The overall crossing probability is very small if considering rare events and thus rather difficult to assess. The key point in TIS is that the overall crossing probability can be expressed as a product of crossing probabilities for the different interfaces λ_s, i.e., $P_A(\lambda_{s+1}|\lambda_s)$ is the probability that whenever λ_s is crossed λ_{s+1} is reached before λ_A. The λ-interfaces can then be adjusted so that the individual crossing probabilities have a reasonable value of 0.05–0.5. For each λ-interface there is a separate path ensemble consisting of trajectories that start in A, cross the corresponding λ-interface, and either go to B or return to A. The flux factor $\langle \phi_0 \rangle$ can be obtained by straightforward MD simulations evaluating the number of positive crossings. Another possibility is to introduce a second path ensemble for the λ_0-interface where the trajectories start outside the stable state, explore the stable state for some time, and end when they leave it. The flux factor is then obtained using the average path length in the two ensembles.[17]

C. Multiple state TPS/TIS

The TPS and especially also the TIS methods work very efficiently for systems exhibiting two distinct stable states. However, for complex systems with several intermediate stable states, trajectories that are supposed to connect the global initial and final states might get stuck in these intermediate states. Since the trajectories are then not returning to either of the two states A or B they do also not contribute to the path ensemble. As a consequence the sampling of pathways becomes very inefficient. To overcome this problem we define a new path ensemble where we include not only pathways that start and end in A or B but all trajectories that connect any two stable states,

$$\mathcal{P}_{\mathrm{MSTPS}}[\mathbf{x}(L)] = \sum_{i,j\neq i} \mathcal{P}_{ij}^{\mathrm{TPS}}[\mathbf{x}(L)], \tag{4}$$

with

$$\mathcal{P}_{ij}^{\mathrm{TPS}}[\mathbf{x}(L)] \equiv Z^{-1} \prod_k \bar{h}_k[\mathbf{x}(L)] h_i(x_0) \mathcal{P}[\mathbf{x}(L)] h_j(x_L). \tag{5}$$

Here we use trajectories with a flexible path length $L\Delta t$, where L denotes the number of slices,[18] i.e., each pathway is stopped as soon as it enters any of the stable states. Z is again a normalization factor

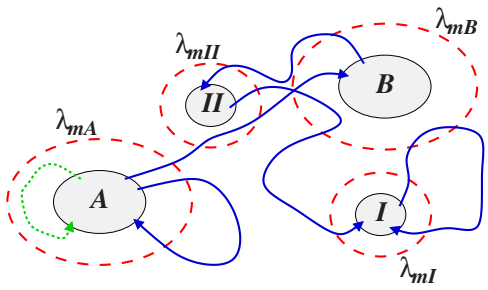

FIG. 1. (Color online) Schematic representation of the multiple state TPS. Every stable state has a set of λ-interfaces up to some outermost λ_m-interface [only λ_m-interfaces (red dashed lines) are shown here]. All pathways that start in one of the stable states cross the corresponding λ_m-interface and end in any of the stable states contribute to the path ensemble [blue (dark) solid trajectories]. Only pathways that return to their initial state without crossing the λ_m-interface will be discarded [green (light) dotted trajectory].

$$Z \equiv \int \mathcal{D}\mathbf{x}(L)\mathcal{P}[\mathbf{x}(L)]\prod_k \bar{h}_k[\mathbf{x}(L)]\sum_{i,j\neq i} h_i(x_0)h_j(x_L), \tag{6}$$

where the integral runs over all paths of all lengths. The different h functions define the stable state regions and ensure that only the end points enter a stable state. The h function defining a stable state can be expressed as

$$h_i(x_\tau) = \begin{cases} 1 & \text{if } x_\tau \in \Lambda_{0i}^- \\ 0 & \text{otherwise,} \end{cases} \tag{7}$$

with the discrete time index $\tau = t/\Delta t$ and $\Lambda_{0i}^- = \{x|\lambda(x) < \lambda_{0i}\}$ [the complementary configuration space is defined as $\Lambda_{0i}^+ = \{x|\lambda(x) > \lambda_{0i}\}$]. Within this notation the λ_{0i}-interfaces are equivalently defined as in TIS (cf. Sec. II B) except that here the index "0i" refers to the λ_0 interface of the state i. Thus, $x_\tau \in \Lambda_{0i}^-$ denotes that the value of the order parameter λ of time slice x_τ, i.e., $\lambda(x_\tau)$, is smaller than the value of the order parameter that defines the stable state i, i.e., λ_{0i}. Since the order parameter has to be a monotonic function it follows that the time slice x_τ is within the stable state region. The flexible path length algorithm demands that all time slices except the first and the last ones are not within any of the stable states. This is achieved by the product over the $\bar{h}$ functions in Eqs. (5) and (6) defined as

$$\bar{h}_i[\mathbf{x}(L)] = \begin{cases} 1 & \text{if } \forall\{\tau|0 < \tau < L\}: x_\tau \notin \Lambda_{0i}^- \\ 0 & \text{otherwise.} \end{cases} \tag{8}$$

Based on the expression for the rate constant in TIS, cf. Eq. (3), we can now also derive an expression for the rate constants between all stable states in the system. For this we assign a set of λ-interfaces to each of the stable states. The corresponding λ order parameter can be different for each stable state and does again not have to correspond to a true reaction coordinate, but still has to clearly distinguish between the respective stable state and all other stable states. In addition, we define an outermost λ-interface, λ_m as shown in Fig. 1. The corresponding TIS path ensemble is then given by

$$\mathcal{P}_{\mathrm{MSTIS}} = \sum_{i,j} \mathcal{P}_{ij}^{\mathrm{TIS}}[\mathbf{x}(L)], \tag{9}$$

with

$$\mathcal{P}_{ij}^{\mathrm{TIS}}[\mathbf{x}(L)] \equiv Z_{\mathrm{TIS}}^{-1}\prod_k \bar{h}_k[\mathbf{x}(L)]h_i(x_0)\mathcal{P}[\mathbf{x}(L)]h_j(x_L)\hat{h}_i^m[\mathbf{x}(L)]. \tag{10}$$

The normalization factor Z is likewise defined as before as the integral over all possible paths of all lengths

$$Z_{\mathrm{TIS}} \equiv \int \mathcal{D}\mathbf{x}(L)\mathcal{P}[\mathbf{x}(L)]\prod_k \bar{h}_k[\mathbf{x}(L)] \times \sum_{i,j} h_i(x_0)h_j(x_L)\hat{h}_i^m[\mathbf{x}(L)], \tag{11}$$

and $\hat{h}_i^m$ is given by

$$\hat{h}_i^m[\mathbf{x}(L)] = \begin{cases} 1 & \text{if } \exists\{\tau|0 \le \tau \le L\}: \ x_\tau \in \Lambda_{mi}^- \\ & \wedge\, \exists\{\tau|0 \le \tau \le L\}: \ x_\tau \in \Lambda_{mi}^+ \\ 0 & \text{otherwise.} \end{cases} \tag{12}$$

Again the two h functions define the stable states i and j and the product over the $\bar{h}$ functions ensures that all time slices except the end points are not in any stable state. In addition the $\hat{h}_i^m$ function restricts the path ensemble to pathways that starting in i and ending in j also cross the corresponding λ_{mi}-interface. Note that the initial and final state can also be the same, i.e., $i=j$ as long as λ_{mi} is crossed, as shown in Fig. 1. In analogy to the TIS method the rate constant for transitions from a state i to a state j can be expressed as

$$k_{ij} = \langle\phi_{mi}\rangle P_i(\lambda_{0j}|\lambda_{mi}). \tag{13}$$

Here $\langle\phi_{mi}\rangle$ is the flux through the λ_{mi}-interface and $P_i(\lambda_{0j}|\lambda_{mi})$ is correspondingly the probability that whenever λ_{mi} is crossed λ_{0j} will be crossed, i.e., state j will be reached, before returning to i. The flux through the outermost interface λ_{mi} can be obtained from a "regular" TIS simulation using the set of λ-interfaces for a given state i,

$$\langle\phi_{mi}\rangle = \langle\phi_{0i}\rangle\prod_{s=0}^{m-1} P_i(\lambda_{(s+1)i}|\lambda_{si}). \tag{14}$$

The crossing probability $P_i(\lambda_{0j}|\lambda_{mi})$ on the other hand is directly obtained from the multiple state transition path ensemble defined in Eq. (9). It is simply given by the number, n_{ij}, of pathways starting in i, crossing λ_{mi} and ending in j divided by all pathways starting in i and crossing λ_{mi},

$$P_i(\lambda_{0j}|\lambda_{mi}) = \frac{\int \mathcal{D}\mathbf{x}(L)\mathcal{P}_{ij}^{\mathrm{TIS}}[\mathbf{x}(L)]}{\int \mathcal{D}\mathbf{x}(L)\sum_j \mathcal{P}_{ij}^{\mathrm{TIS}}[\mathbf{x}(L)]} \approx \frac{n_{ij}}{\sum_j n_{ij}}. \tag{15}$$

From the expression for the rate constants for transitions between all stable states i and j in Eq. (13) it follows that the flux $\langle\phi_{mi}\rangle$ only has to be calculated once for each stable state. All remaining crossing probabilities can be obtained

simultaneously within one multiple state TPS simulation. Since the flux through the λ_{mi}-interface is constant for all transitions out of a certain stable state i the ratio of two rate constants can be expressed as the ratio of the corresponding crossing probabilities,

$$\frac{k_{ij}}{k_{ik}} = \frac{P_i(\lambda_{0j}|\lambda_{mi})}{P_i(\lambda_{0k}|\lambda_{mi})}. \tag{16}$$

One important aspect in the multiple state TPS is that the defined states must be truly metastable in a sense that the system spends so much time in each of these states that transitions between them can be described by a Markov chain. This is important since in this approach a transition $i \to k \to j$ is always described as two independent transitions $i \to k$ and $k \to j$. However this is not a problem as long as all stable states are long lived and transitions between them are rare with respect to the molecular time scale.

D. Algorithm

The first step in the multiple state TPS algorithm is the definition of stable state regions and the corresponding λ_m-interfaces. Starting from some initial trajectory connecting any two states in the system a new pathway is created using a shooting move just as in regular TPS/TIS. For this a shooting point is arbitrarily chosen along the trajectory. If stochastic dynamics are used no changes need to be made at the shooting point, as the stochastic nature of the dynamics is sufficient to obtain a new trajectory. In case of deterministic dynamics within a microcanonical (NVE) ensemble the momenta at the shooting point need to be perturbed to create a new trajectory.[8] The new momenta are correspondingly rescaled to conserve the total momentum and the total energy (an algorithm for sampling the canonical ensemble is also available, see Ref. 8). In both cases the new shooting point can always be accepted. Since we use flexible path length shooting[18] the new trajectory is integrated forward and backward in time until it reaches any of the stable states. The acceptance probability for the new pathway is given by

$$P_{\mathrm{acc}}(\mathbf{x}^{(\mathrm{o})} \to \mathbf{x}^{(\mathrm{n})}) = \prod_k \bar{h}_k[\mathbf{x}^{(\mathrm{n})}(L^{(\mathrm{n})})] \times \sum_{i,j} h_i(x_0^{(\mathrm{n})}) h_j(x_L^{(\mathrm{n})}) \hat{h}_i^m[\mathbf{x}^{(\mathrm{n})}(L^{(\mathrm{n})})] \times \min\left[1, \frac{L^{(\mathrm{o})}}{L^{(\mathrm{n})}}\right]. \tag{17}$$

Thus, a pathway is always accepted if it connects any two stable states and crosses the λ_m-interface of the initial state and if its length fulfills the acceptance criterion due to the flexible path length.[18] In this algorithm reversal moves, i.e., the time reversal of all slices of a path,[8] are not necessary to increase the sampling of the path space since those moves are already implicitly included. This is due to the fact that the trajectories are allowed to start and end in any of the stable states thus including $i \to j$ as well as $j \to i$ pathways.

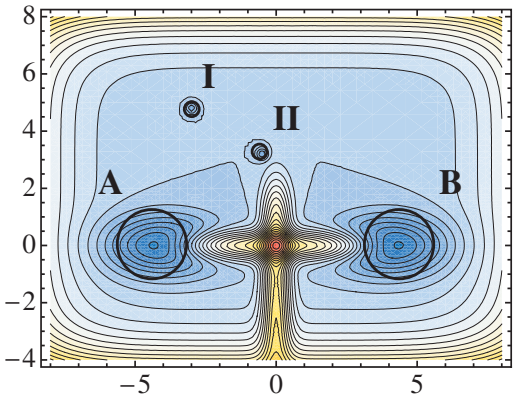

FIG. 2. (Color) 2D model potential for stochastic dynamics. The potential has four minima which are indicated by the black circles. Contour lines correspond to $0.5k_BT$. Transitions can occur between all minima in the system.

III. RESULTS AND DISCUSSION

To illustrate the approach described above we consider two model systems, one using stochastic dynamics in a rather diffusive system and the other one using deterministic dynamics.

A. Model system I: Stochastic dynamics

The model system consists of a simple two-dimensional (2D) potential in which we perform Langevin dynamics (LD). A detailed description of the applied dynamics can be found in Ref. 19. The potential is given by

$$\begin{aligned} V(x,y) = &-4\exp[-0.25(x+4)^2 - y^2] && \min A \\ &-4\exp[-0.25(x-4)^2 - y^2] && \min B \\ &+1/5625[0.0425x^6 + 0.5(y-2)^6] && \text{cutoff} \\ &+5\exp[-4x^2 - 0.01(y+1)^4] && v\text{-barrier} \\ &+5\exp[-0.0081x^4 - 4y^2] && h\text{-barrier} \\ &-2\exp[-20.25((x+3)^2 + (y-4.8)^2)] && \min\ \mathrm{I} \\ &-2\exp[-20.25((x+0.5)^2 + (y-3.2)^2)] && \min\ \mathrm{II}. \end{aligned} \tag{18}$$

This potential has four stable states, two main minima A and B and two intermediate states I and II, as shown in Fig. 2. The stable state regions are defined by circles around the minima with a certain radius r_i which is set to $r_A = r_B = 1.0$ and $r_{\mathrm{I}} = r_{\mathrm{II}} = 0.25$. The corresponding λ-interfaces for each state are defined likewise with λ_{0i} coinciding with the definition of the stable state i. The outermost λ-interfaces are set to $\lambda_{mA} = \lambda_{mB} = 3.0$ and $\lambda_{m\mathrm{I}} = \lambda_{m\mathrm{II}} = 1.0$. In between the stable states the potential is rather flat except for the vertical and horizontal barriers. The vertical barrier is introduced to focus on reactive pathways that pass through the upper part of the potential. The simulations are performed using a friction coefficient of $\gamma = 2.5$, a time step of $\Delta t = 0.1$, and temperatures $\beta = 1/k_BT$ between 1.5 and 4.5. A two-way shooting algorithm with flexible path length is applied resulting in an overall acceptance of ~0.45. To verify the results of the multiple state TPS we compared them to rate constants obtained from

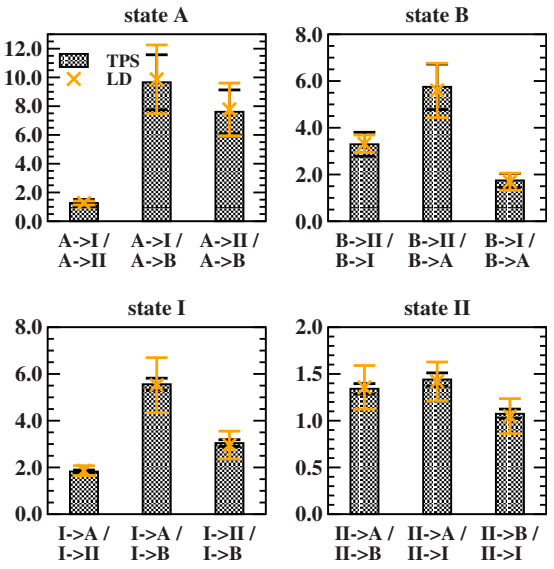

FIG. 3. (Color online) Ratio of the multiple state TPS probabilities $P_i(\lambda_{0j}|\lambda_{mi})/P_i(\lambda_{0k}|\lambda_{mi})$ (gray bars) for the different transitions between the four stable states in the model potential shown in Fig. 2. The temperature is $\beta=2.5$. The orange (light) crosses mark the reference values for the ratio of the corresponding rate constants k_{ij}/k_{ik} obtained from LD simulations.

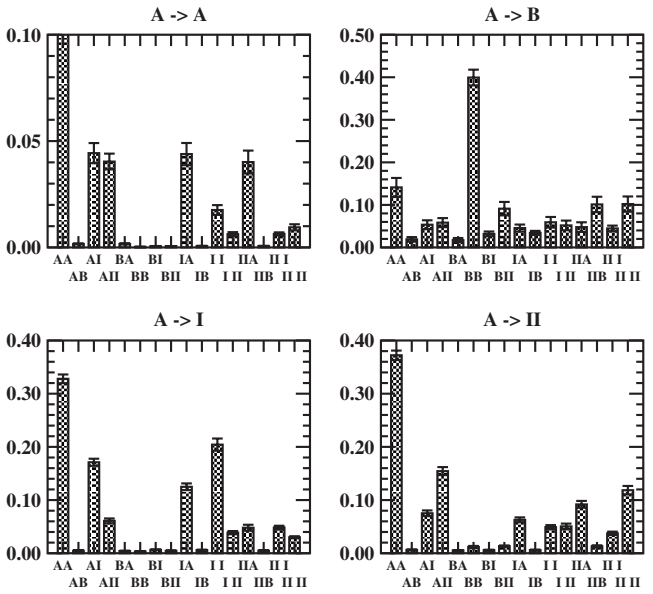

FIG. 4. Correlation between subsequent pathways. The graphs show the fraction of pathways that is created starting from a certain type of pathway. The four graphs show the correlation for pathways originating in state A, i.e., creating new trajectories from $A\rightarrow A$, $A\rightarrow B$, $A\rightarrow$I, and $A\rightarrow$II pathways. For all pathways there is a nonvanishing probability to create any of the other 16 types of pathways.

straightforward LD simulations. As shown in Eq. (16) the ratio of two rate constants for transitions originating from the same stable state can directly be compared to the ratio of the fraction of pathways in the multiple state TPS. The results for a temperature of $\beta=2.5$ are shown in Fig. 3. The error is calculated as the standard deviation over block averages. In the multiple state TPS ten blocks with 10^6 cycles are sampled. The LD rate constants are obtained using the mean first passage time. For each of the four stable states ten blocks with 2000 transitions are counted. To check for a proper sampling of initial conditions within each of the stable states the results are also compared to rate constants obtained using the mean residence times and number of crossing from a long LD trajectory. The results in Fig. 3 show an excellent agreement between the multiple state TPS results and the LD simulations. The trend in the ratios of the different rate constants is as expected from the shape of the potential energy surface (PES). The rate constants for a transition from states $A\rightarrow$I and $A\rightarrow$II are similar whereas the rate constant $A\rightarrow B$ is a factor of $\sim$8 lower. For transitions starting in state B the rate constants $B\rightarrow$I and $B\rightarrow A$ are comparable whereas the rate constant $B\rightarrow$II is a factor of 4–6 larger. Similarly, for state I the rate constants I$\rightarrow A$ and I$\rightarrow$II are comparable and the I$\rightarrow B$ rate constant is somewhat smaller. The very similar rate constants for all three transitions out of minimum II are also consistent with the central position of this state.

The agreement between the multiple state TPS and the LD results is also very good for the other investigated temperatures, i.e., $\beta=1.5$, 3.5, and 4.5. For higher values of β the direct evaluation of the rate constant with LD becomes very costly. For instance, the number of counted transitions per block to determine the mean first passage time is reduced to 1000 for $\beta=3.5$ and to 125 for $\beta=4.5$. At even higher values of β a direct evaluation of the rate constants becomes prohibitively expensive.

The multiple state TPS is most useful in systems with a considerable switching between pathways connecting different stable states, i.e., starting from a pathway $i\rightarrow j$ and applying a shooting move there is certain probability to create a pathway $k\rightarrow l$. To evaluate the switching behavior in the current model system we look at the correlation between subsequent pathways. In Fig. 4 this is shown for pathways originating in state A. Here we plot the fraction of the different possible pathways that is created from an existing one, i.e., looking at the top left graph in Fig. 4 we see that from an $A\rightarrow A$ pathway most likely another $A\rightarrow A$ pathway will be created ($\sim$75%, outside of the shown range in Fig. 4). However there is also a reasonable probability to create trajectories connecting other stable states. This becomes even more obvious at the top right graph in Fig. 4. Here the existing pathway is an $A\rightarrow B$ pathway. The graph shows that $\sim$40% of the subsequent pathways are $B\rightarrow B$ pathways whereas the rest are more or less equally distributed among other types of trajectories. Also for all other pathways we find that there is indeed a nonvanishing probability to create any of the 16 possible pathways from a certain trajectory by a shooting move. If this switching between pathways does not occur a proper sampling of the entire path ensemble might be difficult and for such systems a separate sampling between any two states, as in normal TPS, can be more appropriate. However, from the correlation graphs we can already conclude that for the current potential the multiple state TPS approach is more efficient. In particular the top right graph in Fig. 4 shows that if we would only sample $A\rightarrow B$ trajectories we would have to reject $\sim$98% of all pathways since only 2% of all trajectories created from an $A\rightarrow B$ pathway start and end again in the same states. Even if we would sample all pathways starting in A and ending in any arbitrary state, still the rejection would be $\sim$70%. Since the creation of pathways

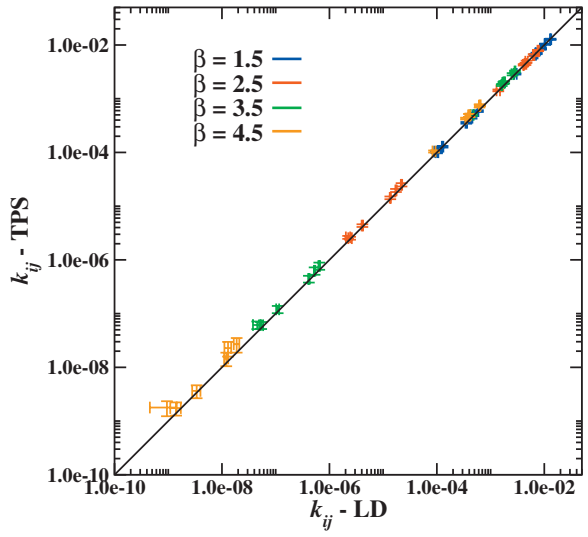

FIG. 5. (Color) Rate constants obtained using the multiple state TPS approach vs rate constants calculated from LD simulations. All rate constants for all 12 possible transitions are shown for four different temperatures.

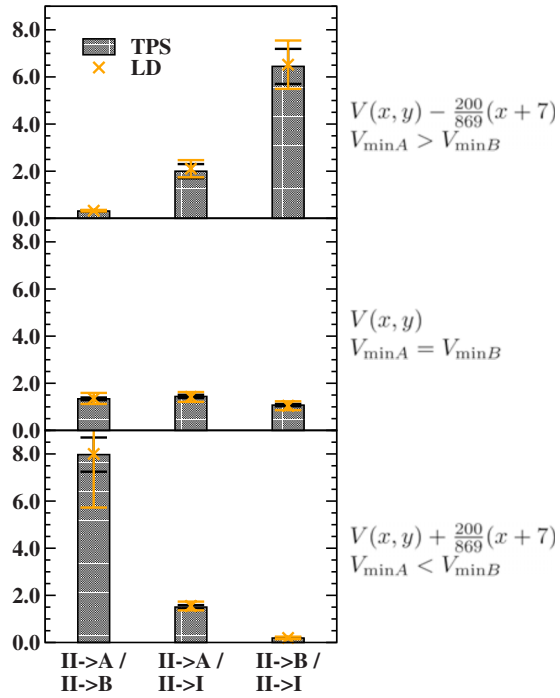

FIG. 6. (Color online) Ratio of the multiple state TPS probabilities $P_i(\lambda_{0j}|\lambda_{mi})/P_i(\lambda_{0k}|\lambda_{mi})$ (gray bars) for the different transitions originating in state II in the model potential shown in Fig. 2 (middle) and in the corresponding tilted potentials, minimum A lower (bottom graph) and higher (top graph) in energy compared to minimum B. The orange (light) crosses mark the reference values for the ratio of the corresponding rate constants k_{ij}/k_{ik} obtained from LD simulations. The temperature is β=2.5.

can become very expensive in large systems it is crucial to discard as few trajectories as possible while still maintaining a good sampling of the path space. Hence, the multiple state TPS can indeed be advantageous in complex systems.

The sampling of the path space can also be analyzed by calculating path correlation functions.[8] For each type of pathway ($A \to A$, $A \to B$, etc.) in the multiple state transition path ensemble we evaluated the path correlation function of an indicator function which is 1 if a certain pathway is sampled and 0 otherwise. A fast decay of the path correlation as a function of shooting moves then indicates a good switching between different pathways, and an efficient sampling of the entire multiple state transition path ensemble. We find that for almost all pathways the path correlation function decays extremely fast, requiring only a few shots (2–8) to fall below a threshold of 0.3. Only for $A \to A$ and $B \to B$ trajectories decorrelation is slightly slower ($\sim$100 shots) which is also reflected in a more frequent sampling compared to other pathways and the switching behavior, as depicted in Fig. 4.

Another factor that can influence the sampling of the path space is the position of the outermost λ_{mi}-interface. As can be seen from Eq. (16) the position of the λ_{mi}-interface does not influence the ratio of the different crossing probabilities out of a given state, but will change the number of pathways that actually return to the stable state after crossing λ_{mi}. If the λ_{mi}-interface is chosen too close to the stable state most of the trajectories will be $i \to i$ pathways and a proper sampling of the entire path ensemble is again not possible. The λ_{mi}-interface can be set arbitrarily far away from the initial stable state, but it must not cross any other stable state nor should it bias the trajectories into a certain part of the phase space. This is trivial for the current 2D model system but might pose a problem in more complex systems.

By performing TIS simulations for each state, we also calculate the flux through all four λ_m-interfaces, and applying Eq. (13), the absolute rate constants. A comparison of the TPS and LD rate constants is shown in Fig. 5. For each temperature we plot the rate constants for all 12 possible transitions in our model system. The rate constants obtained with the two different approaches are in excellent agreement for all applied temperatures. The linear correlation coefficient calculated including all data points is $>$0.99. The presented results clearly confirm that the multiple state TPS approach is valid for the described model system.

To ascertain whether the approach also works on a PES that is not as flat as the one described above we have tilted the original PES, as shown in Fig. 2 by adding a gradient along the x-direction so that minimum A is $2k_BT$ lower (higher) in energy than minimum B,

$$V_{\mathrm{slope}}(x,y) = V(x,y) \pm 200/869(x+7). \tag{19}$$

The results that we obtain on these tilted PESs using the multiple state TPS approach agree likewise very well with the corresponding LD simulations. We also find that the ratio of the crossing probabilities calculated in the multiple state TPS can already provide quite some information regarding the different minima. In Fig. 6 the ratios of the crossing probabilities for all transitions originating in state II are shown for the three different potentials. In the center graph the ratios for the original potential are displayed. Looking at Fig. 2 it appears to be rather obvious that transitions from II$\to A$, II$\to B$, and II$\to$I are equally likely resulting in ratios of about 1. If the PES is tilted so that state A is $2k_BT$ lower in energy than B the ratios change accordingly, cf. bottom graph in Fig. 6. On this tilted PES transitions from state II$\to A$ are much more likely than to state B since once the trajectory has escaped state II there is a downhill slope toward state A but an uphill slope toward state B. The opposite

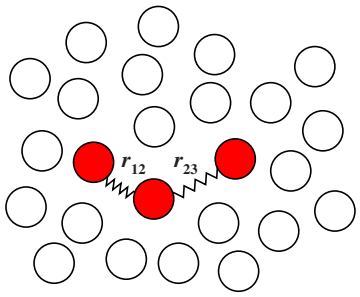

FIG. 7. (Color online) Schematic figure of a triatomic molecule in a WCA fluid. The system contains N particles that interact via the WCA potential. The red (dark) circles indicate the three particles representing the trimer that in addition interact via a double-well potential. Within the system there are four distinct stable states as a function of the interparticle distances between particles 1 and 2 (r_{12}) and particles 2 and 3 (r_{23}).

behavior can be observed in the top graph of Fig. 6 where state A is higher in energy than state B and accordingly the ratios are reversed. Thus if the shape of the PES is unknown already the ratios of the crossing probabilities can provide some useful hints about the relative positions of the different stable states. The results show that even on an uphill potential the multiple state TPS is applicable. Inspection of the fraction of sampled pathways indicates that a good sampling will become more difficult if the transition probabilities between the stable states are very different. On the flat potential $\sim 7\%$ of all pathways are $A \leftrightarrow \mathrm{II}$ pathways. If the potential is tilted toward the B state this number decreases to $\sim 1.5\%$. For transition probabilities that differ by several orders of magnitude the sampling of less likely transitions will indeed become problematic. The sampling of unlikely transitions might be improved by introducing a biasing function which we discuss in Sec. III C 2.

B. Model system II: Deterministic dynamics

To further scrutinize the validity of our approach we apply the multiple state TPS to a second model system now using deterministic dynamics. The model system consists of a trimer surrounded by a fluid, as shown in Fig. 7. The N particles in the system interact via the Weeks–Chandler–Andersen (WCA) potential[20]

$$V_{\mathrm{WCA}}(r) = \begin{cases} 4\epsilon\left[\left(\frac{\sigma}{r}\right)^{12} - \left(\frac{\sigma}{r}\right)^{6}\right] + \epsilon & \text{if } r \le r_{\mathrm{WCA}} \equiv 2^{1/6}\sigma \\ 0 & \text{if } r > r_{\mathrm{WCA}}, \end{cases} \tag{20}$$

where r is the distance between two particles, ϵ specifies the interaction strength, and σ is the interaction radius. The particles in the trimer (particles 1 and 2, respectively, particles 2 and 3) interact in addition via a double-well potential

$$V_{\mathrm{dw}}(r) = h\left[1 - \frac{(r - r_{\mathrm{WCA}} - w)^2}{w^2}\right]^2, \tag{21}$$

where h is the height of the barrier and w is the barrier width. This leads to four distinct stable states in the free energy surface as a function of the interparticle distances r_{12} and r_{23} in the trimer. Due to the double-well potential each of the two interparticle distances can be either in a short (sh), $r=r_{\mathrm{WCA}}$, or in an extended (ex), $r=r_{\mathrm{WCA}}+2w$, configuration, i.e., the four stable states can be described as shsh, exsh, shex, and exex. Transitions are possible between all of the states leading to a total number of 12 transitions. Again we use the multiple state TPS approach to obtain the crossing probabilities and compare this to the corresponding results from straightforward MD simulations. The simulation results are presented in reduced units, i.e., the unit of length is σ, of energy ϵ, of mass m, and of time $\tau \equiv (\sigma^2 m/\epsilon)^{1/2}$. Correspondingly, rate constants are given in units of τ^{-1}. In the simulations the barrier height is set to $h=1.0\epsilon$ and the width to $w=0.25\sigma$. The total number of particles is $N=100$ with a particle density of $\rho=0.6\sigma^{-3}$. Periodic boundary conditions are applied. The simulations are performed in a NVE-ensemble with a total energy of $E=20$, 40, 60, and 80, and 100ϵ corresponding roughly to temperatures of $T=0.171$, 0.335, 0.498, 0.661, and $0.824\epsilon/k_B$, respectively. The equations of motion are integrated using the velocity Verlet algorithm with a time step of $\Delta t=0.001\tau$. In the TPS simulations a two-way shooting algorithm with flexible path length is applied. The maximum momentum displacement at the shooting point is $\delta p_{\max}=5.0(\epsilon m)^{1/2}$ resulting in an overall acceptance of 0.4–0.6. In Fig. 8 a comparison of the ratio of rate constants obtained from MD simulations to the ratio of crossing probabilities obtained from multiple state TPS is shown [cf. Eq. (16)] for a total energy of $E=40\epsilon$. The error bars are calculated as two times the standard deviation over block averages. In the multiple state TPS ten blocks with 5×10^5 cycles each are simulated. The direct evaluation of the rate constants is done by monitoring the number of transitions and mean residence times within the stable states from

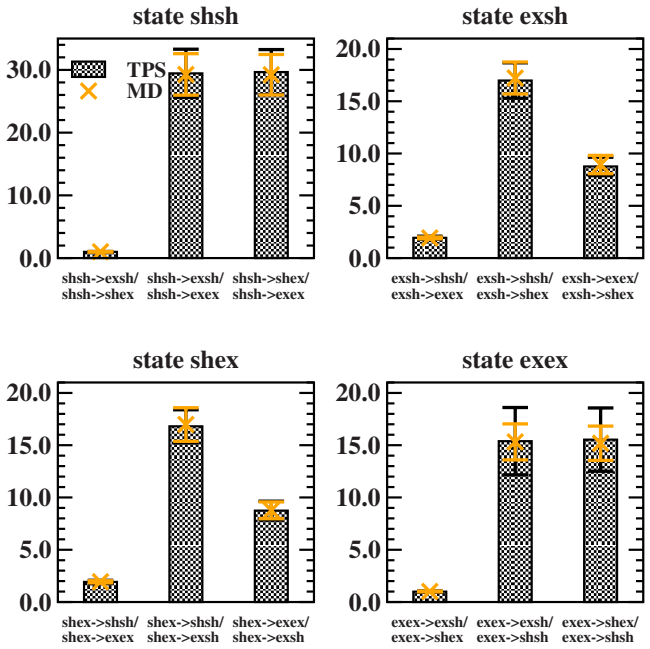

FIG. 8. (Color online) Ratio of the multiple state TPS probabilities $P_i(\lambda_{0j}|\lambda_{mi})/P_i(\lambda_{0k}|\lambda_{mi})$ (gray bars) for the different transitions between the four stable states of the trimer at a total energy of $E=40\epsilon$. The orange (light) crosses mark the reference values for the ratio of the corresponding rate constants k_{ij}/k_{ik} obtained from MD simulations.

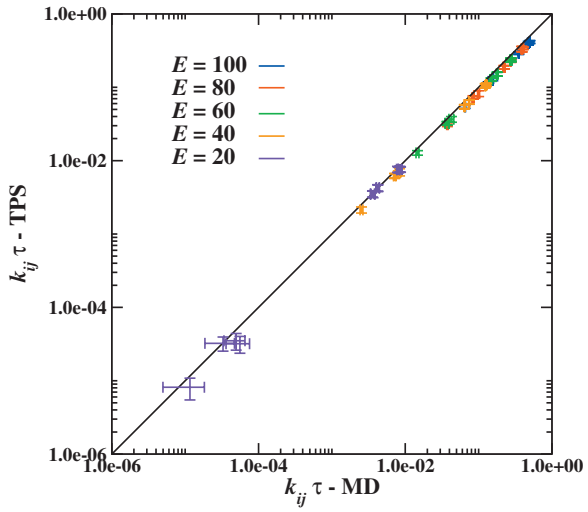

FIG. 9. (Color) Rate constants obtained using the multiple state TPS approach vs rate constants calculated from MD simulations. All rate constants for all 12 possible transitions are shown for five different total energies.

a long MD trajectory with ten blocks of 5×10^8 time steps. Also in this model system using deterministic dynamics, the agreement between the multiple state TPS approach and the straightforward MD simulations is excellent. Looking at the different ratios in Fig. 8 we can immediately see that starting in the shsh-conformation and extending one of the two interparticle distances (shsh→exsh or shsh→shex) is a symmetric process, i.e., the ratio is one. As expected, extending both interparticle distances simultaneously (shsh→exex) has a much lower rate constant (about a factor of 30 at a total energy of 40ϵ). Transitions from the exsh and shex states to a shsh configuration have a two times higher probability than to the exex configuration. This is due to the fact that the free energy of the trimer is slightly lower in the shsh configuration than in the exex configuration due to excluded volume effects. Again, the rate constants for changing both interparticle distances at the same time, i.e., shex→exsh, respectively, exsh→shex, are much smaller. Starting in an exex configuration the same trends as for the shsh state can be observed. To reduce either one of the two interparticle distances is symmetric (exex→shex or exex→exsh) and thus the ratio of the corresponding crossing probabilities is one, while going from exex→shsh is less likely by a factor of 15 (at $E=40\epsilon$).

In addition, we also calculate the flux through the different λ_m-interfaces, and by applying Eq. (13), the total rate constants. A comparison of the rate constants for all possible transitions between the four stable states in the trimer is shown in Fig. 9 for five different total energies. Also for the absolute values of the rate constants we obtain an excellent agreement between the multiple state TPS results and the MD simulations. Again the linear correlation coefficient for the whole data set is >0.99. Based on error estimates we find that for the trimer system the multiple state TPS approach is about ten times as efficient as the separate sampling of each transition with regular two-state TPS.

C. Further developments

There are two main problems that could considerably worsen the sampling of the path space and thus make the multiple state TPS inefficient. One is that the trajectories get stuck in a certain channel in path space and the second one that certain pathways are sampled only very rarely compared to others. Another problem is the identification of all stable states. In the current approach it is assumed that all stable states have been determined *a priori*. In Secs. III C 1 to III C 3 we suggest possible solutions to these problems.

1. Path replica exchange

It has recently been proposed that in normal TIS simulations the sampling of multiple channels can considerably be improved by a replica exchange formalism applied to ensembles of trajectories that belong to different λ-interfaces.[9,17,18] In this approach path replicas belonging to two different ensembles can always be exchanged if they mutually also belong to the ensemble of the other replica.

In the multiple state TPS this can likewise be done for path replicas originating in the same stable state. Trajectories starting in different stable states have a different set of λ-interfaces and can thus not be exchanged. However, if the exchange is combined with a reversal move, i.e., a complete time reversal of the path, then also exchanges between $i\rightarrow j$ and $j\rightarrow i$ pathways are possible. Additionally, in this approach the flux through the different λ_m-interfaces as well as the crossing probabilities are calculated simultaneously.

2. Biasing function

Within the multiple state path ensemble pathways originating in the same stable state are sampled with a probability distribution corresponding to the relative values of the rate constants. Hence trajectories that describe a rather unlikely transition are also sampled rarely. As a consequence a correct sampling of the entire path space might become difficult. Indications concerning the quality of the sampling can, e.g., be obtained by looking at the fraction of different types of pathways,

$$\begin{array}{c|cccc} \rightarrow & A & B & \mathrm{I} & \mathrm{II} \\ A & 0.2853 & 0.0045 & 0.0435 & 0.0343 \\ B & 0.0045 & 0.3242 & 0.0078 & 0.0258 \\ \mathrm{I} & 0.0434 & 0.0078 & 0.0682 & 0.0237 \\ \mathrm{II} & 0.0341 & 0.0255 & 0.0237 & 0.0438 \end{array}. \quad (22)$$

In this matrix the number of $i\rightarrow j$ trajectories divided by the total number of all sampled trajectories are compiled for the first model system at a temperature of $\beta=2.5$. Since within the simulations detailed balance is obeyed the number of pathways $i\rightarrow j$ has to be the same as $j\rightarrow i$ if the sampling is sufficient, resulting in a symmetric matrix. The matrix values show that this is indeed the case for the first model system at $\beta=2.5$, and we also find the same result for all presented systems under various conditions. However, it can also be seen that about 60% of all sampled pathways are $A\rightarrow A$ and $B\rightarrow B$ pathways, whereas only about 0.5% are $A\rightarrow B$ pathways. As discussed above the strong preference for $i\rightarrow i$ tra-

jectories can, e.g., be reduced by placing the λ_m-interface further away from the stable state. This does not change the ratio of the crossing probabilities out of a given state but it decreases the fraction of $i \to i$ pathways, increases the fraction of $i \to j$ trajectories (with $i \neq j$) and correspondingly decreases the flux through the λ_m interface. Having a closer look at the above matrix the fraction of $A \to B$ pathways is still a factor of 10 lower than, e.g., $A \to I$. This ratio though is inherent to the investigated system since it reflects the ratio of the corresponding rate constants, cf. Eq. (16). Hence, depending on the investigated system this ratio might vary over orders of magnitude. Whether the sampling becomes insufficient can be identified from the fraction of pathways. For instance, either the number $i \to j$ and $j \to i$ trajectories are not equal, or a certain type of pathway is sampled so infrequently that the fraction falls within the statistical uncertainty. In such a case a biasing function could be used to increase the sampling of rather unlikely trajectories. The corresponding weight function w_{ij} can be included into the acceptance probability. The value of the weight function can be tuned to the fraction of pathways as listed in the matrix above and might also be updated continuously during the simulation. A slight drawback of this approach is that more pathways will be rejected due to the weighting function. Nevertheless, it can still be efficient since an oversampling of likely transitions can be avoided. Using such a biasing function should enable an equal sampling of all types of trajectories.

3. Identification of new stable states

In the multiple state TPS it is assumed that all stable states are known *a priori*, something that might not always be the case in complex systems. However, a simulation can easily be extended as soon as a new stable state is identified. Within the simulation itself the generation of very long pathways residing in a particular part of the phase space might be used as an indication for additional stable states leading eventually to an automated process for the iterative exploration of the entire path space.

IV. SUMMARY

We have extended the formalism of TPS to include not only two distinct stable states, one initial and one final, but several stable states within a system. In this approach trajectories connecting any two stable states are part of the path ensemble and can be sampled within one simulation. This is crucial for complex processes such as self-assembly of proteins or protein conformational changes where very often, a number of intermediate stable states can be found and transitions between those intermediate states are rare events themselves. Based on the ideas formulated in TIS we derived an expression for the rate constants of all possible transitions between stable states. For the two investigated model systems the results obtained using the multiple state TPS are in excellent agreement with reference values from regular MD simulations. As in all path sampling techniques a proper sampling of the entire path space is essential to obtain correct results. This can only be the case if there is enough switching between pathways with different initial and final states. We have proposed that if the switching is rather low the sampling of unlikely trajectories could be enhanced by introducing a biasing function in the acceptance of pathways. If on the other hand there is no switching at all between different trajectories this part of the path space can as well be sampled using successive two-state TPS/TIS simulations. Thus, for systems where the switching between different states is so pronounced that a two-state sampling is not applicable the multiple state TPS provides a useful alternative. Furthermore, as long as the switching is reasonable the sampling of all transitions within one multiple state TPS simulation is expected to be more efficient since the number of rejected pathways will be lower and also the correlation length between successive pathways is expected to be much shorter than in a two-state TPS simulation. In fact, for the simple systems considered here the multiple state TPS is about an order of magnitude faster. In contrast, if the stable states are not interconnected in phase space or the transition probabilities differ too much a successive two-state sampling will be more efficient. The sampling of the path space is also more difficult if there are several channels between different states that are separated by high barriers. Similar to the approach used in two-state TIS we propose a replica exchange formalism to overcome this problem. Since the multiple state TPS method is straightforward to implement it can easily be applied to proteins or other complex systems to explore multiple stable or metastable states within one simulation.

[1] G. M. Torrie and J. P. Valleau, Chem. Phys. Lett. **28**, 578 (1974).
[2] E. Carter, G. Ciccotti, J. T. Hynes, and R. Kapral, Chem. Phys. Lett. **156**, 472 (1989).
[3] A. F. Voter, J. Chem. Phys. **106**, 4665 (1997).
[4] A. Laio and M. Parrinello, Proc. Natl. Acad. Sci. U.S.A. **99**, 12562 (2002).
[5] J. D. Chodera, W. C. Swope, J. W. Pitera, and K. A. Dill, Multiscale Model. Simul. **5**, 1214 (2006).
[6] J. D. Chodera, N. Singhal, V. S. Pande, K. A. Dill, and W. C. Swope, J. Chem. Phys. **126**, 155101 (2007).
[7] F. Noé, I. Horenko, C. Schütte, and J. C. Smith, J. Chem. Phys. **126**, 155102 (2007).
[8] C. Dellago, P. G. Bolhuis, and P. L. Geissler, Adv. Chem. Phys. **123**, 1 (2002).
[9] T. S. van Erp and P. G. Bolhuis, J. Comput. Phys. **205**, 157 (2005).
[10] D. Moroni, P. R. ten Wolde, and P. G. Bolhuis, Phys. Rev. Lett. **94**, 235703 (2005).
[11] J. Juraszek and P. G. Bolhuis, Proc. Natl. Acad. Sci. U.S.A. **103**, 15859 (2006).
[12] C. Dellago and P. G. Bolhuis, Top. Curr. Chem. **268**, 291 (2007).
[13] M. Grünwald, C. Dellago, and P. L. Geissler, J. Chem. Phys. **127**, 154718 (2007).
[14] M. Grünwald, C. Dellago, and P. L. Geissler, J. Chem. Phys. **129**, 194101 (2008).
[15] C. Dellago, P. G. Bolhuis, and D. Chandler, J. Chem. Phys. **108**, 9236 (1998a).
[16] This Markovian probability should not be confused with the transitions probabilities in the MSM.
[17] T. S. van Erp, Phys. Rev. Lett. **98**, 268301 (2007).
[18] P. G. Bolhuis, J. Chem. Phys. **129**, 114108 (2008).
[19] C. Dellago, P. G. Bolhuis, F. S. Csajka, and D. Chandler, J. Chem. Phys. **108**, 1964 (1998b).
[20] J. D. Weeks, D. Chandler, and H. C. Andersen, J. Chem. Phys. **54**, 5237 (1971).